ELSEVIER

Automation in Construction 9 (2000) 421–435

AUTOMATION IN CONSTRUCTION

www.elsevier.com/locate/autcon

Impedance control of a hydraulically actuated robotic excavator

Q.P. Ha *, Q.H. Nguyen, D.C. Rye, H.F. Durrant-Whyte

Australian Center for Field Robotics, The University of Sydney, J07, Sydney, 2006 NSW, Australia

Abstract

In robotic excavation, hybrid position/force control has been proposed for bucket digging trajectory following. In hybrid position/force control, the control mode is required to switch between position- and force-control depending on whether the bucket is in free space or in contact with the soil during the process. Alternatively, impedance control can be applied such that one control mode is employed in both free and constrained motion. This paper presents a robust sliding controller that implements impedance control for a backhoe excavator. The control law consists of three components: an equivalent control, a switching control and a tuning control. Given an excavation task in world space, inverse kinematic and dynamic models are used to convert the task into a desired digging trajectory in joint space. The proposed controller is applied to provide good tracking performance with attenuated vibration at bucket–soil contact points. From the control signals and the joint angles of the excavator, the piston position and ram force of each hydraulic cylinder for the axis control of the boom, arm, and bucket can be determined. The problem is then how to find the control voltage applied to each servovalve to achieve force and position tracking of each electrohydraulic system for the axis motion of the boom, arm, and bucket. With an observer-based compensation for disturbance force including hydraulic friction, tracking of the piston ram force and position is guaranteed using robust sliding control. High performance and strong robustness can be obtained as demonstrated by simulation and experiments performed on a hydraulically actuated robotic excavator. The results obtained suggest that the proposed control technique can provide robust performance when employed in autonomous excavation with soil contact considerations.

Keywords: Robotic excavator; Hybrid position/force control; Sliding controller

1. Introduction

The usual task of a backhoe excavator is to free and remove material from its original location and to transfer it to another location by lowering the bucket, digging by dragging the bucket through the soil, then lifting, slewing and dumping the bucket. In moving towards automatic excavation, there is a need for the development of a controller that is robust to uncertainties associated with these operations [1]. For control purposes, kinematic and dynamic models of excavators that assume the hydraulic actuators act as infinitely powerful force sources are presented in Refs. [2–4]. Position control with a conventional proportional and derivative controller is used in Refs. [4,5] for simulation of the digging process with limited soil interaction.

Excavators are, however, subject to a wide variation of soil–tool interaction forces. When digging,

* Corresponding author. Department of Mechanics and Mechatronic Engineering, The University of Sydney, J07, 2006 NSW, Australia. Tel.: +61-2-9351-3098; fax: +61-2-9351-7474.

E-mail address: quang.ha@mech.eng.usyd.edu.au (Q.P. Ha).

0926-5805/00/$ - see front matter
PII: S0926-5805(00)00056-X

the bucket tip motion is effectively force-constrained by the nonlinear constitutive equations of the environment, and by the hydraulic forces. Compliance control approaches may therefore be considered to be more suitable than position control for the shaping of excavator dynamics. Compliant motion control can generally be classified into two broad classes: hybrid position/force control and interactive control or impedance/admittance control. In hybrid force/position control, the Cartesian space of the end-effector co-ordinates is decomposed into a position sub-space and a force sub-space. Separate position- and force-trajectory tracking objectives are specified in each sub-space. Excessive force transients may, however, occur at the instant of contact between the tool and the environment. Rather than tracking desired position and force trajectories, interactive control seeks to regulate the relationship between the end-effector position and the interaction force. It is known that impedance control provides a unified approach to both unconstrained and constrained motion [6]. If hybrid position/force control is adopted, the control mode should be switched between position control and force control according to whether the excavator bucket is in free space or in contact with the soil during an excavation task.

Impedance control is believed to be better suited to excavation tasks in the sense that it can be applied continuously to both free and constrained motions [1]. An impedance controller has recently been reported for an excavator arm [7]. This paper proposes a robust sliding mode control technique to implement impedance control for an excavator using generalised excavator dynamics. The bucket tip is controlled to track a desired digging trajectory in the presence of environment and system parameter uncertainties. In impedance control of hydraulic excavators, the piston position and the ram force of each hydraulic cylinder for the axis control of the boom, arm, and bucket can be determined. The problem is then how to find the control voltage applied to the servovalves to track these desired commands. Taking into account friction and nonlinearities, a discontinuous observer is developed for estimating both piston displacement velocity and disturbance including load force and friction. With an observer-based compensation for the disturbance force, robust tracking the piston ram force and position is guaranteed using robust sliding mode controllers for electrohydraulic systems. The validity of the proposed method is verified through simulation and filed tests performed on the Komatsu PC-05 mini-excavator. The remainder of this paper is organised as follows. Section 2 is devoted to the derivation of the excavator dynamic model. The problem formulation and the development of impedance control for excavator dynamics are presented in Section 3. The control of electrohydraulic systems is addressed in Section 4. The hardware organisation for the robotic excavator is described in Section 5 together with computer simulations and experimental results. Finally, conclusions are provided in Section 6.

2. Excavator dynamics

The equations of motion for a generic excavator can be derived by applying the Euler–Lagrange equations to a Lagrangian energy function, or by writing the Newton–Euler equations successively for each link of the machine. In the latter approach, the dynamics of each link are described by equations that recurse through the link index. The driving joint torques of the boom, arm, and bucket are generated by the forces of the hydraulic ram actuators. The translational and rotational motions of these links are described by the dynamic model of the excavator system. Dynamic models of excavators are presented in Ref. [2] with refinements in Ref. [4]. Firstly, a Cartesian co-ordinate frame $\{O_0 x_0 y_0 z_0\}$ fixed to the excavator body is chosen. Other Cartesian co-ordinate frames are systematically assigned by applying the Denavit and Hartenberg procedure as in Refs. [2–4]. The frames $\{O_1 x_1 y_1 z_1\}$, $\{O_2 x_2 y_2 z_2\}$, $\{O_3 x_3 y_3 z_3\}$, and $\{O_4 x_4 y_4 z_4\}$ are respectively attached to the boom, arm, bucket, and bucket tip as seen in Fig. 1.

Note that the movements of the excavator mechanism during digging usually occur in the vertical plane. It is therefore assumed that no boom-swing motion occurs during excavation, so that the boom swing angle θ_1 is therefore held constant ($\theta_1 = 0$) during digging. The model equations can be written for each link of the excavator by considering the link as a rigid free body. By combining Newton and Euler equations for all links, the dynamical model for the excavator can be expressed concisely in a

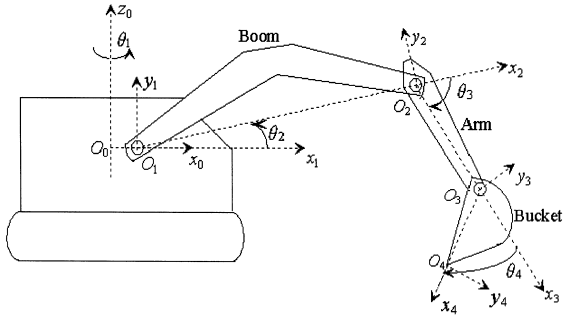

Fig. 1. Excavator joint variables.

well-known form of manipulator equations of motion [4]:

$$\mathbf{D}(\boldsymbol{\theta})\ddot{\boldsymbol{\theta}} + \mathbf{C}(\boldsymbol{\theta},\dot{\boldsymbol{\theta}})\dot{\boldsymbol{\theta}} + \mathbf{B}(\dot{\boldsymbol{\theta}}) + \mathbf{G}(\boldsymbol{\theta}) = \tilde{\mathbf{A}}(\boldsymbol{\theta})\mathbf{F} - \mathbf{T}_{\mathrm{L}}(F_{\mathrm{t}},F_{\mathrm{n}}), \quad (1)$$

where $\boldsymbol{\theta} = [\theta_2 \ \ \theta_3 \ \ \theta_4]^T$ is the vector of measured shaft angles: θ_2 for the boom joint, θ_3 for the arm joint, and θ_4 for the bucket joint; $\mathbf{T}_{\mathrm{L}}$ represents the load torques as functions of the tangential and normal components, F_{t} and F_{n}, of the soil reaction force at the bucket, and $\mathbf{F}$ are the ram forces of the hydraulic actuators that produce the torques acting on the joint shafts. The tangential component, F_{t}, which is parallel to the digging direction, represents the resistance to the digging of ground by excavators bucket teeth. This resistance is considered as the sum of soil's resistance to cutting, the friction between the bucket and the ground, and the resistance to movement of the prism of soil and soil movement in the bucket. The tangential component can be calculated according to Ref. [8] as

$$F_{\mathrm{t}} = k_1 bh, \quad (2)$$

where k_1 is the specific digging force [N m^{-2}], and h and b are respectively the thickness and width of the cut slice of soil [m]. The normal component, F_{n}, is calculated as

$$F_{\mathrm{n}} = \Psi F_{\mathrm{t}}, \quad (3)$$

where $\psi = (0.1\text{–}0.45)$ is a factor depending on the digging angle, digging conditions, and the wear and tear of the cutting edge [8]. The determination of the matrices of inertia, $\mathbf{D}(\boldsymbol{\theta})$, of Coriolis and centripetal effects, $\mathbf{C}(\boldsymbol{\theta},\dot{\boldsymbol{\theta}})\dot{\boldsymbol{\theta}}$, of gravity forces, $\mathbf{G}(\boldsymbol{\theta})$, and of functions of the moment arms, $\tilde{\mathbf{A}}(\boldsymbol{\theta})$, is comprehensively described in Refs. [2–4]. All entries in these matrices are given in Ref. [4]. The 3×1-matrix of viscous friction $\mathbf{B}(\dot{\boldsymbol{\theta}})$ is treated in this paper as a source of uncertainty.

In the digging plane, the Jacobian $\mathbf{J}(\boldsymbol{\theta})$ defined as

$$\dot{\boldsymbol{x}} = \mathbf{J}(\boldsymbol{\theta})\dot{\boldsymbol{\theta}}, \quad (4)$$

can be obtained from Ref. [3], where $\boldsymbol{x} = [x_4 \ \ z_4 \ \ \theta_{O_4}]^T$ represents the Cartesian co-ordinates and orientation of the bucket tip (O_4) with respect to $\{O_0\, x_0\, y_0\, z_0\}$. Assuming that the Jacobian matrix $\mathbf{J}(\dot{\boldsymbol{e}})$ is non-singular, Eq. (1) in joint space can be rewritten in Cartesian space as:

$$\mathbf{H}(\boldsymbol{x})\ddot{\boldsymbol{x}} + \mathbf{C}_x(\boldsymbol{x},\dot{\boldsymbol{x}})\dot{\boldsymbol{x}} + \mathbf{B}_x(\dot{\boldsymbol{x}}) + \mathbf{G}_x(\boldsymbol{x}) = \mathbf{J}^{-T}\tilde{\mathbf{A}}\mathbf{F} - \mathbf{F}_{\mathrm{e}}, \quad (5)$$

where

$$\mathbf{H} = \mathbf{J}^{-T}\mathbf{D}\mathbf{J}^{-1}, \quad \mathbf{C}_x = \mathbf{J}^{-T}(\mathbf{C} - \mathbf{D}\mathbf{J}^{-1}\mathbf{J})\mathbf{J}^{-1},$$
$$\mathbf{G}_x = \mathbf{J}^{-T}\mathbf{G}, \quad \mathbf{B}_x = \mathbf{J}^{-T}\mathbf{B}, \quad (6)$$

and $\mathbf{F}_{\mathrm{e}} = \mathbf{J}^{-T}\mathbf{T}_{\mathrm{L}}$ denotes the generalised forces of interaction between the end-effector (bucket tip) and the environment (soil). They consist of digging forces acting on the bucket with force entries for the co-ordinates (x_4, z_4) and a torque entry around y_4.

The determination of the forward and inverse kinematic relationships, $\boldsymbol{x} = \mathbf{L}(\boldsymbol{\theta})$ and $\boldsymbol{\theta} = \mathbf{L}^{-1}(\boldsymbol{x})$ is detailed in Ref. [3]. As Eq. (5) has the form of the generalised robotic manipulator dynamics where $\boldsymbol{x}$ is a vector of the co-ordinates of the contact point of the manipulator with the environment, below and in the next section, we will consider in general $\boldsymbol{x} \in R^n$ and $\boldsymbol{u} \in R^n$. We assume

$$\text{A1: } \mathbf{H} = \hat{\mathbf{H}} + \ddot{\mathbf{A}}\mathbf{H}, \quad \mathbf{C}_x = \hat{\mathbf{C}}_x + \Delta\mathbf{C}_x,$$
$$\mathbf{G}_x = \hat{\mathbf{G}}_x + \Delta\mathbf{G}_x, \quad \tilde{\mathbf{A}} = \tilde{\mathbf{A}} + \Delta\tilde{\mathbf{A}}, \quad \mathbf{F}_{\mathrm{e}} = \hat{\mathbf{F}}_{\mathrm{e}} + \Delta\mathbf{F}_{\mathrm{e}}, \quad (7)$$

where matrices $\hat{\mathrm{H}}$, $\hat{\mathrm{C}}_x$, $\hat{\mathrm{G}}_x$, and $\tilde{\mathbf{A}}$ are known, $\hat{\mathbf{F}}_{\mathrm{e}}$ is to be measured by force sensors such as load pins, and $\Delta\mathbf{H}$, $\Delta\mathbf{C}_x$, $\Delta\mathbf{G}_x$, $\Delta\tilde{\mathbf{A}}$, and $\Delta\mathbf{F}_{\mathrm{e}}$ are uncertainties.

Denoting friction and uncertainties by

$$\Delta\mathbf{f}(\ddot{\boldsymbol{x}},\dot{\boldsymbol{x}},\boldsymbol{x}) = \Delta\mathbf{H}\dot{\boldsymbol{x}} + \Delta\mathbf{C}_x\dot{\boldsymbol{x}} + \Delta\mathbf{G}_x + \mathbf{B}_x\dot{\boldsymbol{x}} + \Delta\mathbf{F}_{\mathrm{e}} - \mathbf{J}^{-T}\Delta\tilde{\mathbf{A}}\mathbf{F}, \quad (8)$$

Eq. (5) can be rewritten as

$$\hat{\mathbf{H}}(\boldsymbol{x})\ddot{\boldsymbol{x}} + \hat{\mathbf{C}}_x(\boldsymbol{x},\dot{\boldsymbol{x}})\dot{\boldsymbol{x}} + \hat{\mathbf{G}}_x(\boldsymbol{x}) = \boldsymbol{u} - \hat{\mathbf{F}}_e - \Delta\mathbf{f}(\ddot{\boldsymbol{x}},\dot{\boldsymbol{x}},\boldsymbol{x}), \quad (9)$$

where

$$\boldsymbol{u} = \mathbf{J}^{-T}\tilde{\mathbf{A}}\mathbf{F} \quad (10)$$

is the control input.

Remark 1. As $\mathbf{D}(\boldsymbol{\theta})$ is a 3×3-symmetric positive-definite matrix satisfying the skew symmetric property [9], for the nominal dynamics ($\Delta\mathbf{f}(\ddot{\boldsymbol{x}},\dot{\boldsymbol{x}},\boldsymbol{x}) = 0$) of the excavator, $[\hat{\dot{\mathbf{H}}}(\boldsymbol{x})\text{-}2\hat{\mathbf{C}}_x(\boldsymbol{x},\dot{\boldsymbol{x}})]$ is also a skew-symmetric matrix, i.e.

$$\boldsymbol{x}^T\left[\hat{\dot{\boldsymbol{H}}}(\boldsymbol{x}) - 2\hat{\mathbf{C}}_x(\boldsymbol{x},\dot{\boldsymbol{x}})\right]\boldsymbol{x} = 0, \qquad \forall\boldsymbol{x}. \quad (11)$$

3. Excavator dynamics impedance control

3.1. Problem formulation

One of the excavating task elements is penetration of the soil by an excavator bucket to follow a pre-planned digging trajectory. During digging, three main tangential resistance forces arise: the resistance to soil cutting, the frictional force acting on the bucket surface in contact with the soil, and the resistance to movement of the prism of soil ahead of and in the bucket. The magnitude of the digging resistance forces depends on many factors such as the digging angle, volume of the soil prism, volume of material ripped into the bucket, and the specific resistance to cutting. These factors are generally variable and unavailable. Moreover, due to soil plasticity, spatial variation in soil properties, and potential severe inhomogeneity of material under excavation, it is impossible to exactly define the force needed for certain digging conditions.

The objective of impedance control is to establish a desired dynamical relationship between the end-effector (bucket tip) position and the contact force. This dynamical relationship is referred to as the *target impedance*. Let $\boldsymbol{x}_r(t)$ be the desired trajectory of the end-effector. Typically, the target impedance is chosen as a linear second-order system to mimic mass-spring-damper dynamics:

$$\mathbf{Z}_t(s)e_{\mathrm{P}} = \left(\mathbf{M}_t s^2 + \mathbf{B}_t s + \mathbf{K}_t\right)e_{\mathrm{P}} = \mathbf{M}_t\ddot{e}_{\mathrm{P}} + \mathbf{B}_t\dot{e}_{\mathrm{P}} + \mathbf{K}_t e_{\mathrm{P}} = e_{\mathrm{F}}, \quad (12)$$

where s is the derivative operator and the constant positive-definite $n\times n$-matrices $\mathbf{M}_t$, $\mathbf{B}_t$ and $\mathbf{K}_t$ are respectively the matrices of inertia, damping and stiffness. The position error, e_{P}, and the force error, e_{F}, are defined as

$$e_{\mathrm{P}} = \boldsymbol{x}_r - \boldsymbol{x}, \quad e_{\mathrm{F}} = \mathbf{F}_r - (-\mathbf{F}_{\mathrm{e}}), \quad (13)$$

where $\mathbf{F}_r(t) = \mathbf{M}_t\ddot{\boldsymbol{x}}_r + \mathbf{B}_t\dot{\boldsymbol{x}}_r + \mathbf{K}_t\boldsymbol{x}_r$ is the force set-point.

The control problem is to asymptotically drive the system state to implement the target impedance (12) even in the presence of uncertainty. If the position error e_{P} approaches zero, the force error e_{F} also approaches zero and vice versa, according to a specified dynamical relationship defined by the numerical values of the matrices $\mathbf{M}_t$, $\mathbf{B}_t$ and $\mathbf{K}_t$ in Eq. (12). In some contact tasks, the force set-point, $\mathbf{F}_r$, will be specified to be constant rather than time-varying. During free-space motion where there is no contact with the environment, $\mathbf{F}_r = -\mathbf{F}_{\mathbf{e}} = 0$, so e_{P} tends to zero since $\mathbf{Z}_t(s) = \mathbf{M}_t s^2 + \mathbf{B}_t s + \mathbf{K}_t$ is stable. The choice of the matrices $\mathbf{M}_t$, $\mathbf{B}_t$ and $\mathbf{K}_t$ will determine the shape of the desired transient response of the system. When the end-effector contacts the environment, the interaction is characterised by the target impedance (12), which results in a compromise between the position error and the force error. If the end-effector position tracks the desired trajectory ($\boldsymbol{x}\to\boldsymbol{x}_r$) then the contact force follows the force set-point ($-\mathbf{F}_{\mathbf{e}}\to\mathbf{F}_r$).

3.2. Controller development

Consider a manipulator dynamical model of the form (5) with uncertainty satisfying condition (7). It is well known [10] that robustness is the most distinguished feature of variable structure control with sliding mode. In this section, a robust sliding mode controller will be developed for the manipulator dynamics (5). As Eq. (5) represents a $2n$-dimen-

sional system with an *n*-dimensionalcontrol input, a sliding surface in the state space will be a manifold of dimension $2n - n = n$ [10]. Let us define $\mathbf{s} = [s_1(\boldsymbol{x}),\ s_2(\boldsymbol{x}),\ldots,\ s_n(\boldsymbol{x})]^T$, the sliding functions, as follows [11]:

$$\mathbf{s} = -\dot{e}_{\mathrm{P}} - \mathbf{M}_t^{-1}\mathbf{B}_t e_{\mathrm{P}} - \mathbf{M}_t^{-1}\mathbf{K}_t\int e_{\mathrm{P}}\mathrm{d}\tau + \mathbf{M}_t^{-1}\int e_{\mathrm{F}}\mathrm{d}\tau = \dot{\boldsymbol{x}} - \dot{\boldsymbol{x}}_s, \tag{14}$$

where

$$\dot{\boldsymbol{x}}_s = \dot{\boldsymbol{x}}_r + \mathbf{M}_t^{-1}\mathbf{B}_t e_{\mathrm{P}} + \mathbf{M}_t^{-1}\mathbf{K}_t\int e_{\mathrm{P}}\mathrm{d}\tau - \mathbf{M}_t^{-1}\int e_{\mathrm{F}}\mathrm{d}\tau. \tag{15}$$

The existence of a sliding mode, $\boldsymbol{s} = 0$, requires that

$$\dot{\mathbf{s}} = -\ddot{e}_{\mathrm{P}} - \mathbf{M}_t^{-1}\mathbf{B}_t\dot{e}_{\mathrm{P}} - \mathbf{M}_t^{-1}\mathbf{K}_t e_{\mathrm{P}} + \mathbf{M}_t^{-1}e_{\mathrm{F}} = 0. \tag{16}$$

It can be seen that once the system state is in the sliding mode associated with Eq. (14), condition (16) guarantees that the target impedance (12) is reached. Thus, in the sliding mode $s_i(\boldsymbol{x}) = 0$, $(i = 1,2,\ldots,n)$, the force error tends to zero. The magnitudes $|s_i(\boldsymbol{x})|$ $(i = 1,2,\ldots,n)$ represent then the deviations of the system state from the sliding surface. We assume further that:

A2: Each entry of the uncertainty $\Delta\mathbf{f}(\ddot{\boldsymbol{x}},\dot{\boldsymbol{x}},\boldsymbol{x})$ is bounded:

$$|\Delta f_i(\ddot{\boldsymbol{x}},\dot{\boldsymbol{x}},\boldsymbol{x})| \le \beta_i, \quad \forall(\ddot{\boldsymbol{x}},\dot{\boldsymbol{x}},\boldsymbol{x}) \qquad (i = 1,2,\ldots,n). \tag{17}$$

Let us now define the control input

$$\boldsymbol{u} = \hat{\boldsymbol{u}} - \mathbf{Q}\,\mathrm{sgn}(\mathbf{s}), \tag{18}$$

where

$$\hat{\boldsymbol{u}} = \hat{\mathbf{H}}\ddot{\boldsymbol{x}}_s + \hat{\mathbf{C}}_x\dot{\boldsymbol{x}}_s + \hat{\mathbf{G}}_{\boldsymbol{x}} + \hat{\mathbf{F}}_{\mathrm{e}}, \tag{19}$$

$$\mathbf{Q} = \left[Q_1\,\mathrm{sgn}(s_1),\ldots,Q_n\,\mathrm{sgn}(s_n)\right]^T, \quad Q_i > \beta_i \qquad (i = 1,2,\ldots,n). \tag{20}$$

Remark 2. The control law (18) consists of two components. The component (19), calculated with the nominal system dynamic model, is called the *equivalent control*. The other component, with the discontinuous gain given in Eq. (20), is called the *switching control*.

Theorem 1. *Consider the system of Eq. (5) associated with sliding functions (14) and the target impedance (12). If the assumptions A1 and A2 are satisfied, and the control law (18) is employed, then the impedance error (14) asymptotically converges to zero [9].*

Implementation implies that sufficiently large switching gains, Q_i, are available. Large values of Q_i will, however, tend to excite chattering. To accelerate the reaching phase and to reduce chattering, the control law (18) is added by a tuning component:

$$\boldsymbol{u} = \hat{\boldsymbol{u}} - \mathbf{Q}\,\mathrm{sgn}(\mathbf{s}) - \mathbf{K}\mathbf{s}, \tag{21}$$

where

$$\mathbf{K} = \mathrm{diag}\left[K_i(s_i)\right] \qquad (i = 1,2,\ldots,n). \tag{22}$$

Employing the fuzzy tuning technique proposed in Ref. [12], the expressions for $K_i(s_i) > 0$ are chosen as:

$$K_i = K_{i\max}\left[1 - \exp\left(-|s_i|/\delta_i\right)\right] \qquad (i = 1,2,\ldots,n), \tag{23}$$

where $K_{i\max}$ and δ_i are some positive constants.

Theorem 2. *Consider the system of Eq. (5) associated with the sliding functions (14) and the target impedance (12). If the assumptions A1 and A2 are satisfied, and the control law (21) is employed then the impedance error (14) asymptotically converges to zero [9].*

Remark 3. The switching component is for ensuring robust stability only. It can be omitted in practice.

Note that from the geometry of the excavator, there exists a trigonometric mapping between each joint angle θ_i and the corresponding linear displacement y_i of each hydraulic cylinder piston, $i = 2,3,4$ [13]. Using this relationship and Eq. (10), the cylinder positions $\mathbf{y} = [y_2\ y_3\ y_4]^T$ and the ram forces $\mathbf{F}$ of the hydraulic actuators can be determined. They are considered as the control references to the excavator hydraulic systems. The following section is devoted to the control of electrohydraulic systems in order to track these desired commands.

4. Electrohydraulic systems control

4.1. Hydraulic modelling

The control (10) requires the ram force generated at each cylinder of the excavator arms follow a desired function of time when executing digging tasks in impedance control. Nonlinear effects occurring during the tool–soil interaction, and in the hydraulic system itself, complicate the control strategy requirements. It is known that gravitational and friction between the piston and cylinder should be compensated for to achieve high performance of heavy-duty hydraulic machines, such as excavators [13]. Furthermore, oil viscosity, oil flow through the hydraulic servovalve, and variable loading, will cause hydraulic control systems to suffer from highly nonlinear time-variant dynamics, load sensitivity, and parameter uncertainty [14]. Thus, these factors have to be taken into account in servo hydraulic modelling and control. The hydraulic actuators incorporated in the blade, boom swing, boom, arm, and bucket attachments of the excavator are axial hydraulic cylinders. The flow of hydraulic oil to the cylinder is regulated by a direct drive servovalve with an electrically controlled closed loop that controls spool position. This system could be generally described by a six-order differential equation. For simplicity, the following linear expression can be used with little loss of accuracy for frequencies up to 200 Hz:

$$x_v = K_v u_v, \tag{24}$$

where x_v is the spool valve displacement and u_v is the valve input voltage. Thus, a nonlinear state model can be obtained as in Ref. [15], based on the relationship between the valve displacement x_v and the fluid flow to the head side Q_1 and from the rod side Q_2, the continuity of flow in the cylinder, and the force balance equation for the piston:

$$\dot{y} = v$$

$$\dot{v} = \frac{1}{M}\left[A_1 P_1 - A_2 P_2 - F_L\right]$$

$$\dot{P}_1 = \frac{\beta_e}{A_1 y + V_h}\left\{Ku_v\left[s(x_v)\sqrt{P_S - P_1} + s(-x_v)\sqrt{P_1}\right] - C_{ip}(P_1 - P_2) - A_1 v\right\}$$

$$\dot{P}_2 = \frac{-\beta_e}{A_2(L-y) + V_h}\left\{Ku_v\left[s(x_v)\sqrt{P_2} + s(-x_v)\sqrt{P_S - P_2}\right] + C_{ip}(P_1 - P_2) - A_2 v\right\}, \tag{25}$$

where y is the piston displacement [m], v is its velocity, P_1 and P_2 are respectively the fluid pressures at the head and rod sides of the cylinder [Pa], u_v is the control input [V], F_L is a load disturbance on cylinder including external forces and friction [N], P_S is the supply pressure [Pa], K is a fixed constant, M is the equivalent moving mass [kg], C_{ip} is the internal leakage coefficient, A_1 and A_2 are respectively the area of the piston head and rod [m^2], V_h is the hose volume between the servovalve and the cylinder [m^3], and $s(x_v)$ is a switching function depending on the extension or retraction of the piston [15]:

$$s(x_v) = \begin{cases} 1 & x_v \geq 0 \\ 0 & x_v < 0 \end{cases}. \tag{26}$$

By assigning the ram force

$$\mathbf{F} = A_1 P_1 - A_2 P_2 \tag{27}$$

as a state variable, an equivalent form of Eq. (25) can be obtained as follows

$$\dot{y} = v$$

$$\dot{v} = \frac{1}{M}\left[\mathbf{F} - F_L\right]$$

$$\dot{\mathbf{F}} = a_{12} v + a_{13}\mathbf{F} + a_{14} P_1 + b_1 u_v$$

$$\dot{P}_1 = a_{22} v + a_{23}\mathbf{F} + a_{24} P_1 + b_2 u_v \tag{28}$$

where

$$a_{12} = -\left(\frac{A_1^2 \beta_e}{A_1 y + V_h} + \frac{A_2^2 \beta_e}{A_2(L-y) + V_h}\right),$$

$$a_{13} = -\left(\frac{A_1/A_2}{A_1 y + V_h} + \frac{1}{A_2(L-y) + V_h}\right)\beta_e C_{ip},$$

$$a_{14} = a_{13}(A_2 - A_1),$$

$$a_{22} = -\frac{A_1^2 \beta_e}{A_1 y + V_h}, \quad a_{23} = -\frac{1/A_2}{A_1 y + V_h}\beta_e C_{ip},$$

$$a_{24} = a_{23}(A_2 - A_1),$$

$$b_1 = \frac{A_1 \beta_e K}{A_1 y + V_h}\left[s(x_v)\sqrt{P_S - P_1} + s(-x_v)\sqrt{P_1} \right] + \frac{A_2 \beta_e K}{A_2(L-y) + V_h} \times \left[s(x_v)\sqrt{P_2} + s(-x_v)\sqrt{P_S - P_2} \right],$$

$$b_2 = \frac{A_1 \beta_e K}{A_1 y + V_h}\left[s(x_v)\sqrt{P_S - P_1} + s(-x_v)\sqrt{P_1} \right]$$

In Eq. (28), information of the states can be obtained from the piston position and pressure transducers. Our experiments indicated, however, that differential pressure readings would be inadequate when used to represent the external force **F** exerted on the hydraulic piston. Taking static friction into account, load pins inserted at the cylinder rod eyes are used for force measurements in our mini-excavator for a more accurate representation of the force **F**. The piston velocity, v, and load disturbance F_L will be estimated using a discontinuous observer as described in the next section. Numerical values of parameters for the excavator arm-axis hydraulic control system can be found in Ref. [16].

4.2. Discontinuous observer for disturbance estimation

In tracking control of electrohydraulic manipulators, there is a need to compensate for the influence of external disturbance such as the acting force coming from outside the hydraulic cylinder, gravity, and friction. Hydraulic servos are affected by a variety of frictional forces including linear and nonlinear viscous frictions and Coulomb friction. An adaptive nonlinear observer [17] is proposed to compensate for Coulomb friction in tracking control of a manipulator actuated by a linear hydraulic cylinder. Simultaneous estimation of velocity and Coulomb friction [15] is obtained via the observer where velocity is estimated independently using a first order low-pass filtered differentiator and static friction is taken into consideration using an approximation model. Variable structure control theory has brought a new insight to nonlinear observers in terms of high insensitivity to uncertainties [18]. It is from this merit that a discontinuous observer is developed to provide robust estimate of the piston velocity and disturbance force. Assuming that the disturbance force is slowly time-varying, the state model for can be written with y as the output,

$$\dot{v} = w - F_L, \quad \dot{F}_L = 0, \quad \dot{y} = v, \tag{29}$$

where w is the acting force measured by a force sensor. Note that in Ref. [17], w denotes the force due to all sources other than friction. In our application, the ram force (27), measured from load pins, is used for estimating external disturbance F_L.

The Utkin observer [19] for Eq. (29) can be designed to have the schematic diagram shown in Fig. 2, where $\sigma = \mu\ \mathrm{sgn}(e_y)$ with $\mu > 0$, $e_y = \hat{y} - y$ is the output error, and the circumflex (^) denotes the estimates. The convergence rate of the proposed observer depends on a proper choice of the observer gains l_1, l_2, or, in other words, on selecting eigenvalues of the following observer characteristic equation [20]:

$$s^2 - l_1 s + l_2 = 0. \tag{30}$$

In order to reduce chattering associated with the sliding motion of the output error, the signum function $\sigma = \mu\ \mathrm{sgn}(e_y)$ is replaced by a sigmoidal one

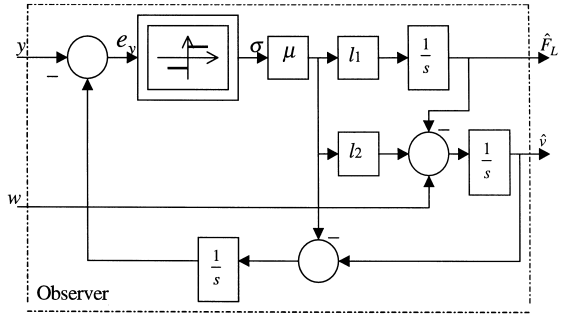

Fig. 2. Observer schematic diagram.

resulted from a fuzzy reasoning technique presented in Ref. [21]:

$$\sigma = \mu \tanh(e_y/\gamma_e) \tag{31}$$

where γ_e is some positive constant.

4.3. Hydraulic controller design

Various advanced control methods addressing the electrohydraulic servo control problem have been reported in literature. Among these methods, variable structure control with a sliding mode has been promoted by many authors [22,23]. The reason is mainly because of its robustness to uncertainties. This section describes the design of a chattering-attenuated sliding mode controller that provides robust tracking of the desired ram force $\mathbf{F}_r$ and piston position y_r required to implement impedance control of the excavator bucket tip in the presence of soil uncertainties. Let us define the control errors

$$e_1 = y - y_r, \quad e_2 = v - v_r, \quad e_3 = \mathbf{F} - \mathbf{F}_r,$$
$$e_4 = P_1 - P_{1r}, \tag{32}$$

where v_r and P_{1r} are respectively the desired piston velocity and head-side fluid pressure. Assuming that estimates of the piston velocity and disturbance force obtained from the observer are adequately accurate, from Eqs. (28) and (32), the following nonlinear dynamics can be derived for the error vector $\boldsymbol{e} = [e_1\ e_2\ e_3\ e_4]^T$:

$$\dot{\boldsymbol{e}} = \mathbf{A}(\boldsymbol{x}, \boldsymbol{x}_r) + \mathbf{B}(u + f), \tag{33}$$

where

$$\mathbf{A}(\boldsymbol{x}, \boldsymbol{x}_r) = \begin{pmatrix} \hat{v} - v_r = e_2 \\ \dfrac{\mathbf{F} - \hat{F}_L}{M} - \dot{v}_r = \dfrac{e_3 - \hat{F}_L}{M} \\ a_{12}\hat{v} + a_{13}\mathbf{F} + a_{14}P_1 - \dot{\mathbf{F}}_r \\ a_{22}\hat{v} + a_{23}\mathbf{F} + a_{24}P_1 - \dot{P}_{1r} \end{pmatrix},$$

$$\mathbf{B} = \begin{pmatrix} 0 \\ 0 \\ b_1 \\ b_2 \end{pmatrix}, \tag{34}$$

and f is an uncertain source taking into account parameter variations and modelling mismatch.

A3: It is assumed that f is unknown but bounded by a known positive function ρ_{sw}:

$$|f| \le \rho_{sw}. \tag{35}$$

Let us now define the following switching function

$$S = \mathbf{C}\mathbf{e} = e_3 + c_2 e_2 + c_1 e_1, \tag{36}$$

where $\mathbf{C} = [c_1\ c_2\ 1\ 0]$ and c_i $(i = 1,2)$ are positive constants to be specified according to the desired dynamics of the closed-loop system. From Eq. (34), it can found that the sliding mode $S = 0$ is associated with the eigenvalues of the following characteristic equation:

$$\frac{1}{M}s^2 + c_2 s + c_1 = 0. \tag{37}$$

Remark 4. With the choice of the sliding function (36), the undesirable influence of the pressure error e_4 can be excluded from the servovalve control voltage u_v.

A necessary condition for the state trajectory to stay on the sliding modes $S = 0$ is $\dot{S} = 0$. The following control law

$$u_v = u_{eq} + u_{sw} + u_{ft} \tag{38}$$

is proposed [24]. It consists of three components: an equivalent control u_{eq} to assign desired dynamics to the closed-loop system, a switching control u_{sw} to guarantee a sliding mode, and a fuzzy control u_{ft} to enhance fast tracking and to attenuate chattering. The equivalent control can be obtained from the nominal system parameters, denoted with bars $(-)$, as follows [12,24]:

$$u_{eq} = -(\mathbf{CB})^{-1}(\mathbf{CA})$$
$$= -\bar{b}_1^{-1}\left[(c_1 + \bar{a}_{12})\hat{v} + \left(\frac{c_2}{M} + \bar{a}_{13}\right)\right.$$
$$\left.\times\mathbf{F} + \bar{a}_{14}P_1 - r - \frac{c_2}{M}\hat{F}_L\right], \tag{39}$$

Fig. 3. Teleoperated robotic excavation.

where $r = c_1\dot{\mathbf{x}}_r + c_2\ddot{\mathbf{x}}_r + \dot{\mathbf{F}}_r$ and the coefficients c_i ($i = 1,2$) are chosen according to the desired roots of the characteristic equation (Eq. (37)). In order to force the system trajectory back to the sliding mode in the presence of uncertainties and to smooth out the control action, the switching and fuzzy control [24] are proposed:

$$u_{\text{sw}} = -\rho_{\text{sw}}\,\text{sgn}(\varphi), \tag{40}$$

$$u_{\text{ft}} = -u_{\text{fm}}\tanh(\varphi/\gamma_t), \tag{41}$$

where $\varphi = S\mathbf{CB} = Sb_1$, and u_{fm} and γ_t are some positive constants.

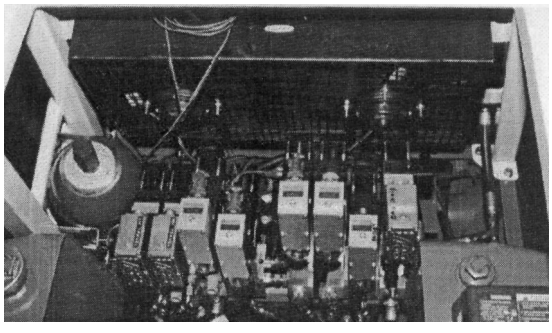

Fig. 4. Electrohydraulic servovalves.

Remark 5. The law (39) can be considered as a combination of state feedback and feedforward con-

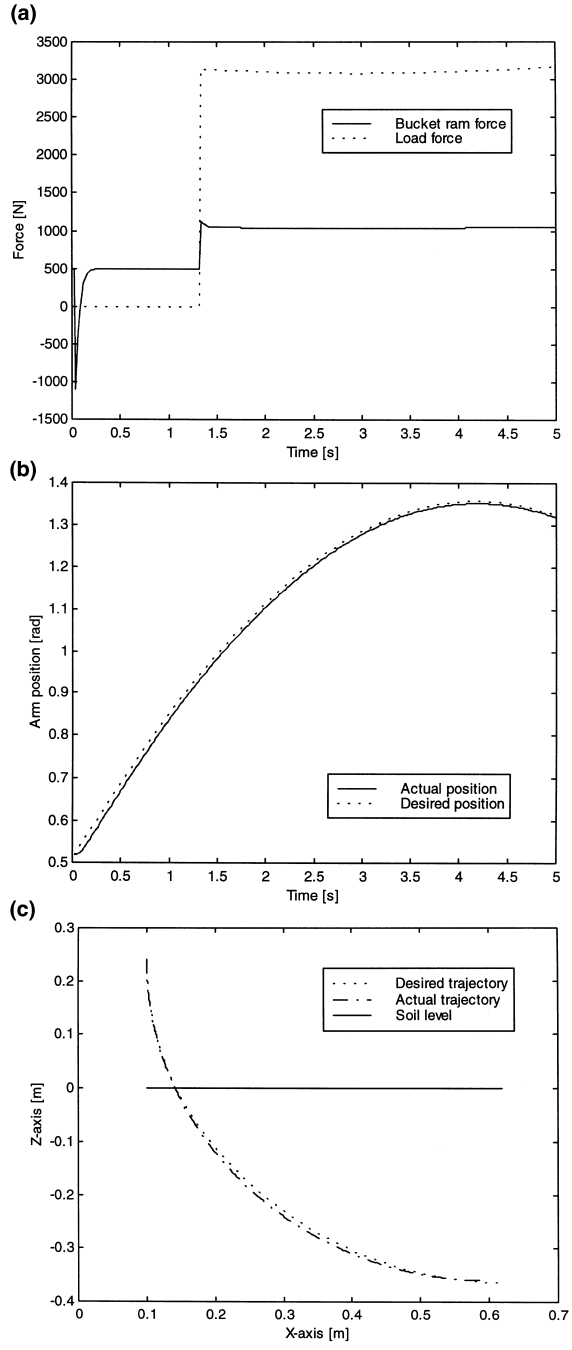

Fig. 5. Digging responses.

trol. Experience shows that the observer dynamics (30) should be chosen three to five times as faster as the system dynamics (37).

5. Simulation and field test results

5.1. The robotic mini-excavator

Fig. 3 shows the robotic excavator used for experiments. The machine, originally a 1.5-tonne Komatsu PC05-7 mini-excavator, has been retrofitted with electrohydraulic servovalves (Fig. 4), spool valve position and pressure transducers, 12-bit joint angle encoders, and digital axis controllers. Additional ancillary equipment needed to support the servovalves is also fitted: an accumulator with unloading valve, solenoid check valves and an air radiator. The machine has eight hydraulic axes: two rubber tracks, cab slew, arm swing, boom, arm, bucket, and a small blade for back filling.

Closed-loop control of all axes is achieved by four proprietary programmable digital controllers that are commanded and coordinated by an industrial IBM-compatible personal computer (PC). The PC communicates with the digital controllers through a (control area network) (CAN) bus, and issues track velocity commands and axis position set-points. At this time, system motion commands are inputted via a joystick that is interfaced to the PC.

5.2. Simulation results

The matrices of inertia, damping and stiffness of the target impedance (12) are chosen respectively as $\mathbf{M}_t = 100\mathbf{I}_3$, $\mathbf{B}_t = 5000\mathbf{I}_3$, $\mathbf{K}_t = 10\,000\mathbf{I}_3$, where $\mathbf{I}_3$ is the 3×3 identity matrix. The controller parameters for Eq. (21) are $\mathbf{Q} = 0$, $K_{i\ \max} = 1000$, $\delta_i = 20$ ($i = 1,2,3$). The soil model used in the simulation is ''sandy loam'' with characteristic parameters given in Ref. [25]. For the multi-axis control of the excavator arm, the desired eigenvalues of Eq. (37) are chosen at $\{-10, -10\}$, which gives a settling time of 0.4 s and no overshoot. The controller parameters for electrohydraulic systems are: $l_1 = -70$, $l_2 = 2500$, $\mu = 5$, $\gamma_e = 0.01$, $c_1 = 100$, $c_2 = 20$, $\rho_{\text{sw}} = 3$, $u_{\text{fm}} = 3$, and $\gamma_t = 0.1$.

The proposed impedance controller is applied to a position tracking process when the bucket is in free space and in force-constrained motion. A desired

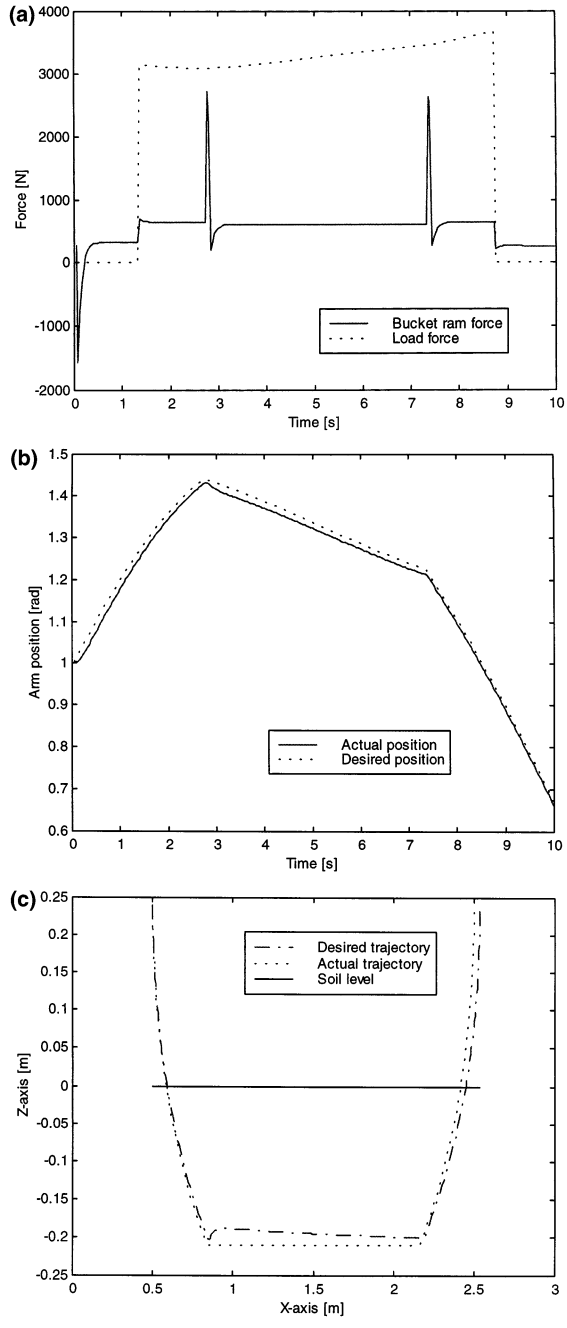

Fig. 6. Responses to a planned digging trajectory.

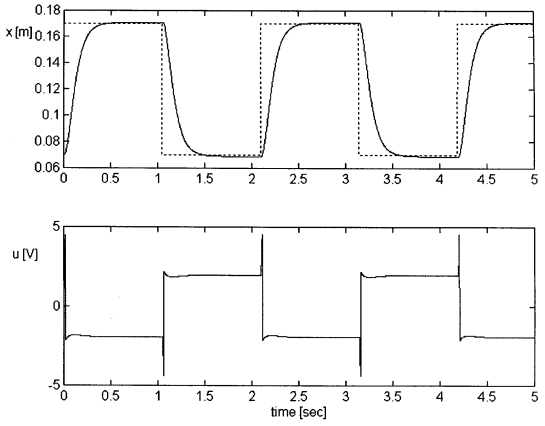

Fig. 7. Rotary cutting tracking responses.

trajectory is first specified in Cartesian space. The inverse kinematic equations of the excavator [3] are used to calculate the desired joint trajectories. Consider first the soil reaction during the digging process when the bucket contacts the soil and begins to penetrate the surface. Fig. 5 shows the load force and bucket ram force; the arm joint angle; and the x–z trajectory. As changes to the bucket–soil contact conditions may result in tracking oscillations, it seems prudent to choose large values for the damping matrix $\mathbf{B}_t$ in the target impedance. Good tracking performance is exhibited during both free motion and constrained motion. Oscillations and errors in the joint angles at the instant of contact with the soil are significantly suppressed. Now let us simulate the task of collecting a bucket of ''sandy loam'' by controlling the excavator in such a way that the bucket follows a given trajectory in a predefined posture. The trajectory template used in the simulation can be considered as a penetrate–drag–curl motion. Fig. 6 depicts the responses of the bucket ram force and load force, the arm position, and the planned trajectory and bucket trajectory. As presented in Ref. [2], significant vibrations in joint angular positions, velocities and accelerations occur at the points where the bucket begins to penetrate the surface or when it is removed from the surface when employing a pure position controller. With the use of an impedance controller, it is seen that these oscillations can be substantially reduced.

In impedance control of the robotic excavator, our objectives focus on the execution of common excavation tasks such as digging building footings, or loading haul trucks from an open-cut mine bench. For our experimental mini-excavator, the digging force for a cut depth of about 0.2 m into ''sandy loam'' can be estimated [25] to be about 3.4 kN.

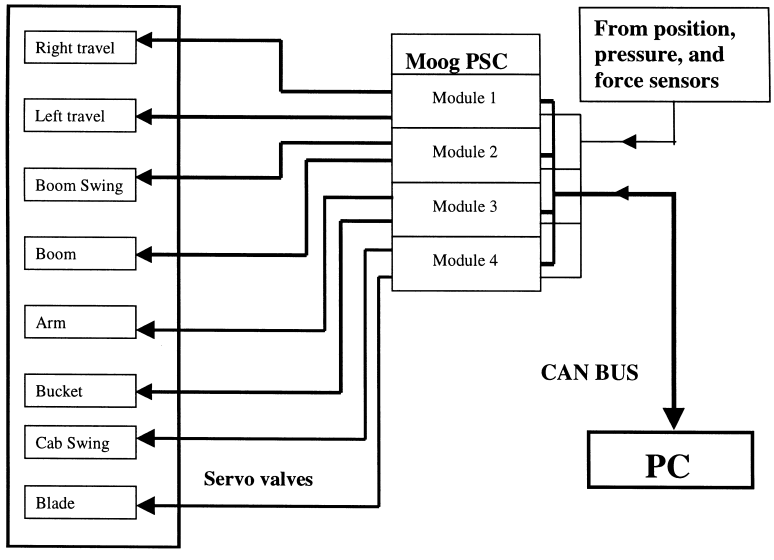

Fig. 8. Hardware organisation.

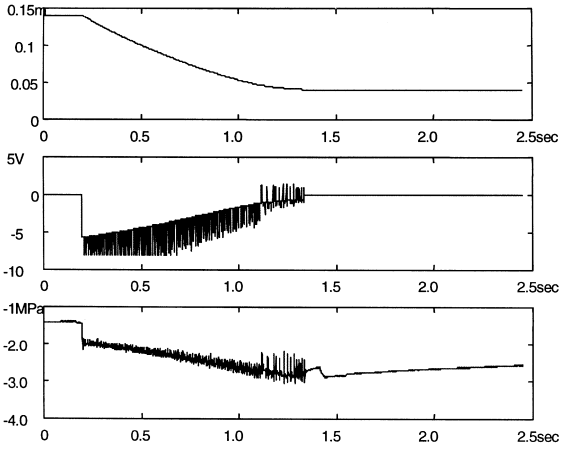

Fig. 9. Experimental free motion responses.

When rotary cutting with the excavator arm, the arm cylinder piston has to track square motion sequences between 0.07 and 0.17 m. The cylinder position and the servovalve control voltage responses of the arm hydraulic system are shown in Fig. 7. It can be seen that robust tracking and a significant reduction of chattering are obtained with the proposed control scheme.

It should be noted that here, the force exerted by the excavator on the soil is controlled not by regulating the position error nor the force error but through the imposed relationship (Eq. (12)) between them.

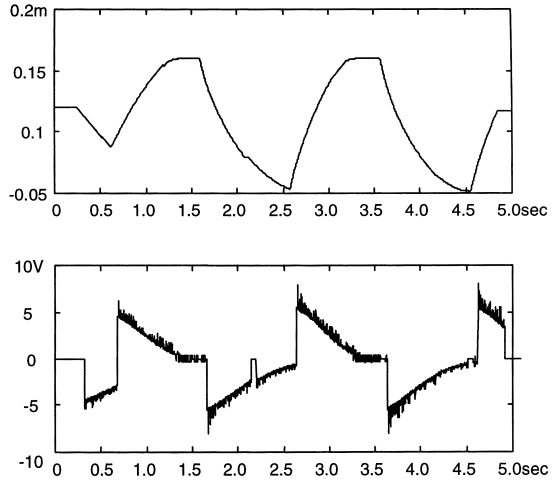

Fig. 10. Experimental tracking responses when digging ‘‘sandy loam’’.

The simulations illustrate that the proposed control schemes can perform adequately in an autonomous excavating task.

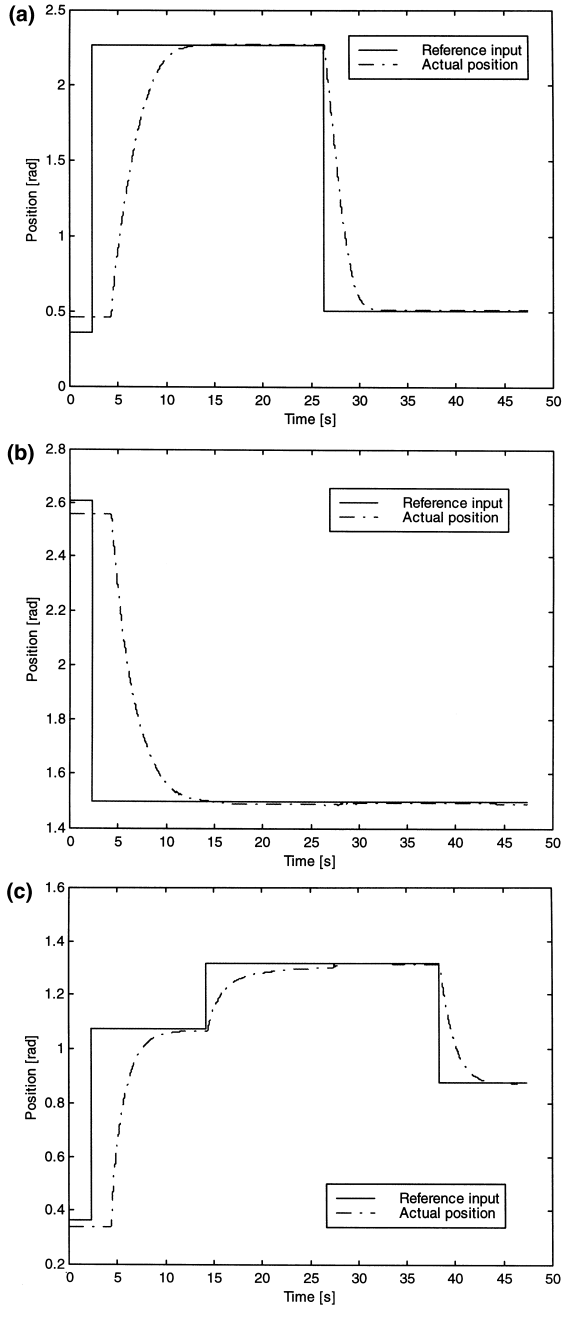

Fig. 11. Loading a truck with impedance control: (a) bucket, (b) arm, and (c) boom joint angles.

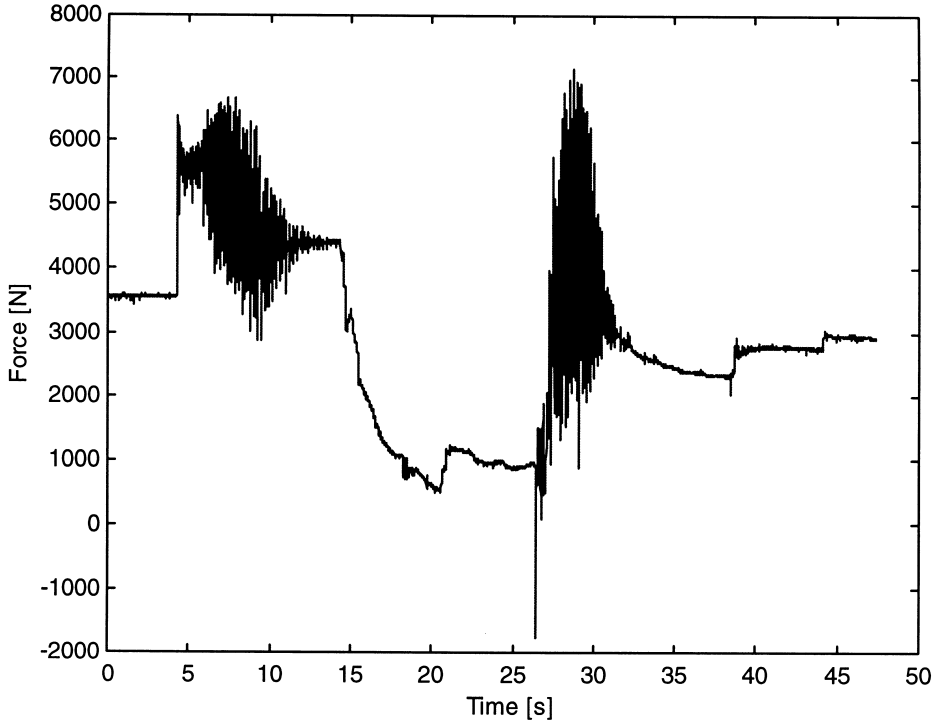

Fig. 12. Bucket ram force during a truck loading task.

5.3. Experimental results

Experiments have been performed on the Komatsu PC05-7 mini-excavator shown in Fig. 3. The hardware organisation of electrohydraulic systems for axis control of to implement impedance control for excavator dynamics is presented in Fig. 8. Data acquisition and control algorithms are written in C + + and executed under the Windows NT operating system. The sampling time is chosen to be 0.010 [s]. The CAN bus communication rate is set at 250 [kBit/s].

The arm position, valve voltage, and load pressure responses in free space with the use of the proposed sliding mode controller are depicted in Fig. 9. Very accurate tracking can be observed. To demonstrate robust tracking in constrained motions, Fig. 10 shows the arm position and valve control voltage responses when digging ''sandy loam'' according to a prescribed target impedance (12) of the bucket tip.

Let us now consider the excavation task of loading a truck. With the target impedance (12), the reference and actual responses the boom, arm, and bucket joint positions are respectively shown in Fig. 11. The ram force exerting at the bucket joint during the excavation task is represented in Fig. 12 for one loading pass, i.e. digging and unloading the soil. The results obtained verified the validity and feasibility of our proposed robust control schemes for autonomous operations of the robotic excavator taking into account tool–soil interactions.

6. Conclusion

In moving towards autonomous excavation in the mining, earth moving and construction industries, we have proposed a robust sliding mode controller for impedance control of excavators dealing with uncertainties in its dynamical model, friction and bucket–soil interactions. The controller design consists of the

choice of a target impedance, and the determination of an equivalent control, a switching control, and a tuning control. The control outputs and the joint angles are then converted to the commands, namely the desired ram force and piston position, to the axis control of electrohydraulic servo systems of the excavator. Sliding mode control incorporating a fuzzy tuning approach has been successfully implemented for the control of the ram force and the cylinder position the excavator hydraulic actuators. A 1.5-tonne robotic mini-excavator is simulated and experimentally tested to verify the validity of the proposed control schemes. Given a desired trajectory, excavating tasks such as digging and loading exhibit good performance. Vibrations in joint angular positions, velocities and accelerations due to the contact between the bucket and the soil can be significantly reduced using the proposed controllers. High performance and strong robustness of the excavator electrohydraulic servo systems are achieved in simulation and field tests. The results obtained demonstrate the feasibility and efficacy of the proposed technique for the control of excavator dynamics and its hydraulic actuators in execution of robotic excavation tasks with soil contact considerations.

Acknowledgements

The support of the Australian Research Council, of NS Komatsu, and of the Co-operative Research Centre for Mining Technology and Equipment is gratefully acknowledged.

References

[1] A.T. Le, Q.H. Nguyen, Q.P. Ha, D.C. Rye, H.F. Durrant-Whyte, M. Stevens, V. Boget, Towards autonomous excavation, in: Proceedings of the International Conference on Field and Service Robotics FSR'97, Canberra, Australia, 1997, pp. 121–126.

[2] P.K. Vaha, M.J. Skibniewski, Dynamic model of an excavator, J. Aerosp. Eng. 6 (2) (1993) 148–158.

[3] A.J. Koivo, Kinematics of excavators (backhoes) for transferring surface material, J. Aerosp. Eng. 7 (1) (1994) 17–31.

[4] A.J. Koivo, M. Thoma, E. Kocaoglan, J. Andrade-Cetto, Modeling and control of excavator dynamics during digging operation, J. Aerosp. Eng. 9 (1) (1996) 10–18.

[5] P.K. Vaha, M.J. Skibniewski, Cognitive force control of excavators, J. Aerosp. Eng. 6 (2) (1993) 159–166.

[6] N. Hogan, Impedance control: an approach to manipulation: Part I. Theory, Part II. Implementation, Part III. Applications, ASME J. Dyn. Syst., Meas., Control 107 (1985) 1–24.

[7] S.E. Salcudean, S. Tafazoli, K. Hashtrudi-Zaad, P.D. Lawrence, Evaluation of impedance and teleoperation control of a hydraulic mini-excavator, in: Proceedings of the 5th Int. Sym. Experimental Robotics ISER'97, Barcelona, Spain, 1997, pp. 187–198.

[8] T.V. Alekseeva, K.A. Artem'ev, A.A. Bromberg, R.L. Voitsekhovskii, N.A. Ul'yanov, in: Machines for earthmoving work, theory and calculations, A.A. Balkema, Rotterdam, 1986.

[9] Q.P. Ha, Q.H. Nguyen, D.C. Rye, H.F. Durrant-Whyte, Robust impedance control of excavator dynamics, in: Proceedings of the International Conference on Field and Service Robotics FSR'99, Pittsburgh, USA, 1999, pp. 226–231.

[10] J.Y. Hung, W. Gao, J.C. Hung, Variable structure control: a survey, IEEE Trans. Ind. Electron. 40 (1) (1993) 2–21.

[11] Z. Lu, A.A. Goldenberg, Robust impedance control and force regulation: theory and experiment, Int. J. Robotics Res. 14 (3) (1995) 225–254.

[12] Q.P. Ha, Sliding performance enhancement with fuzzy tuning, IEE Electron. Lett. 33 (16) (1997) 1421–1423.

[13] S. Tafazoli, P.D. Lawrence, S.E. Salcudean, D. Chan, S. Bachmann, C.W. de Silva, in: Parameter estimation and actuator friction analysis for a mini-excavator, Proceedings of the Int. Conf. on Robotics and Automation ICRA'96, Minneapolis, USA, 1996, pp. 329–334.

[14] H.E. Merritt, in: Hydraulic Control Systems, Wiley, New York, 1976.

[15] S. Tazafoli, C.W. de Silva, P.D. Lawrence, Tracking control of an electrohydraulic manipulator in the presence of friction, IEEE Trans. Control Systems Technol. 6 (3) (1998) 401–411.

[16] Q.H. Nguyen, Q.P. Ha, D.C. Rye, H.F. Durrant-Whyte, Feedback linearisation control for electrohydraulic systems of a robotic excavator, in: Proceedings of the Australian Conference on Robotics and Automation (ACRA 99), Brisbane, Australia, 1999, pp. 190–195.

[17] B. Friedland, Y.J. Park, On adaptive friction compensation, IEEE Trans. Autom. Control 37 (10) (1992) 1609–1612.

[18] C. Edwards, S.K. Spurgeon, On the development of discontinuous observers, Int. J. Control 59 (5) (1994) 1211–1229.

[19] V.I. Utkin, in: Sliding Modes in Control Optimisation, Springer-Verlag, 1992, pp. 206–222.

[20] Q.P. Ha, Q.H. Nguyen, D.C. Rye, H.F. Durrant-Whyte, Force and position control for electrohydraulic systems of a robotic excavator, in: Proceedings of the IAARC/IFAC/IEEE International Symposium on Automation and Robotics in Construction ISARC '99, Madrid, Spain, 1999, pp. 483–489, (ISARC '99 best paper).

[21] Q.P. Ha, D.C. Rye, H.F. Durrant-Whyte, Fuzzy moving sliding mode control with application to robotic manipulators, Automatica 35 (4) (1999) 607–616.

[22] C.L. Hwang, C.H. Lan, The position control of electro-hydraulic servomechanism via a novel variable structure control, Mechatronics 4 (4) (1994) 369–391.
[23] I. Tunay, O. Kaynak, Provident control of an electro-hydraulic servo with experimental results, Mechatronics 6 (3) (1996) 249–260.
[24] Q.P. Ha, D.C. Rye, H.F. Durrant-Whyte, Robust sliding mode control with application, Int. J. Control 72 (12) (1999) 1087–1096.
[25] A.N. Zelenin, V.I. Balovnev, I.P. Kerov, in: Machines for Moving the Earth, A.A. Balkema, Rotterdam, 1987, (Translation from Russian).